Photon Counting and Energy Discriminating X-Ray Detectors - Benefits and Applications

David WALTER [1], Uwe ZSCHERPEL [1], Uwe EWERT [1]
[1] BAM Bundesanstalt für Materialforschung und -prüfung, Berlin, Germany

Contact e-mail: david.walter@bam.de

Abstract. Since a few years the direct detection of X-ray photons into electrical signals is possible by usage of highly absorbing photo conducting materials (e.g. CdTe) as detection layer of an underlying CMOS semiconductor X-ray detector. Even NDT energies up to 400 keV are possible today, as well.

The image sharpness and absorption efficiency is improved by the replacement of the unsharp scintillation layer (as used at indirect detecting detectors) by a photo conducting layer of much higher thickness.

If the read-out speed is high enough (ca. 50 – 100 ns dead time) single X-ray photons can be counted and their energy measured. Read-out noise and dark image correction can be avoided. By setting energy thresholds selected energy ranges of the X-ray spectrum can be detected or suppressed. This allows material discrimination by dual-energy techniques or the reduction of image contributions of scattered radiation, which results in an enhanced contrast sensitivity. To use these advantages in an effective way, a special calibration procedure has to be developed, which considers also time dependent processes in the detection layer. This contribution presents some of these new properties of direct detecting digital detector arrays (DDAs) and shows first results on testing fiber reinforced composites as well as first approaches to dual energy imaging.

Introduction

Since many years classical film radiography is being replaced by digital detector imaging especially in medicine applications due to faster and more reliable diagnostics and computed tomography and tomosynthesis capabilities. In the field of non-destructive testing digital detector imaging via imaging plates (IPs) and digital detector arrays (DDAs) is becoming more and more important due to the same reasons as in medical applications.

Moreover, within the large field of digital radiography the method of detecting X-rays is becoming diverse, as well. Besides indirect detection of X-rays using IPs and DDAs with scintillation layers (e.g. CsI), the direct detection by DDAs based on semiconductor monocrystals (e.g. Si, GaAs or CdTe) is gaining more and more importance in NDT applications. If equipped with fast read-out electronics (ASICs), those direct detecting DDAs can be run in photon counting mode which allows detecting single photons and even determining their energies. Hence, those photon counting detectors (PCDs) offer multiple advantages compared to indirect detecting DDAs. Low image unsharpness and high contrast sensitivity are the most obvious ones. Furthermore, the energy discriminating capability of the PCDs can be used for materials separation purposes.

1. Technology

1.1 Principle

Common indirect detecting technology is based on scintillation layers (e.g CsI) which convert incident X-ray photons into visible light that is detected by photodiodes (see Figure 1). As the conversion into light is diffuse, the scattered light leads to an inner unsharpness of the scintillation layer which blurs the image. To limit the inner unsharpness scintillation layers are often quite thin (50 – 400 µm) and therefore not very efficient.

Direct detecting detectors are based on semiconductor mono-crystallites which convert incident X-ray photons into electron-hole pairs which can be directly detected by the electric in a strong electrical field read-out circuit. As there is no considerable scattering of light or electrons in the detection process itself, the thickness of the monocrystals, and therefore the detective quantum efficiency, can be improved without loss in image sharpness. Common thicknesses of CdTe based photon counting detectors vary by 0.75 - 2 mm.

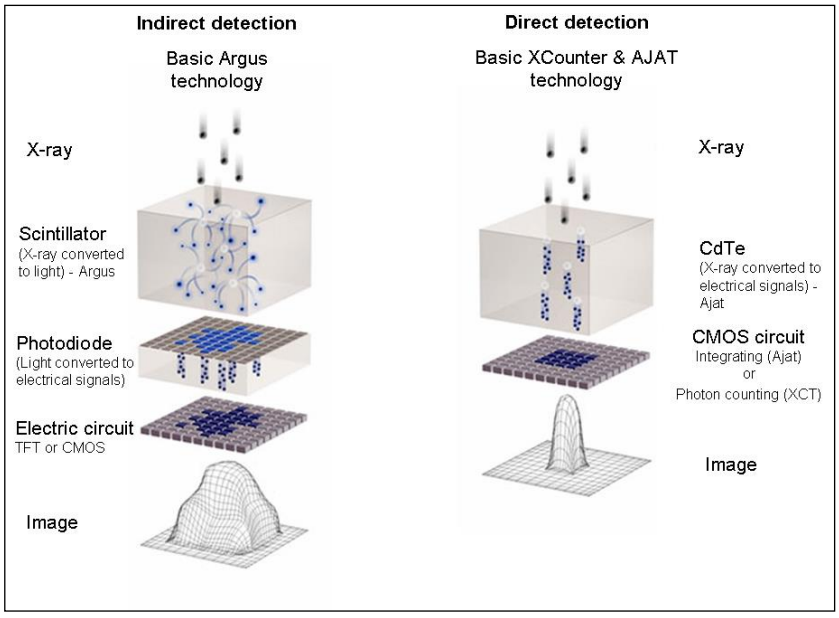

Figure 1: Comparison between indirect (left) and direct (right) detection of X-rays [1]

When direct X-ray detection technology is combined with fast read-out circuits (allowing dead times of about 50 – 100 ns) single photons can be counted at typical X-ray exposure conditions. Each photon deposits a certain charge proportional to its energy inside of the crystal. When comparing this charge to one or more pre-defined thresholds a classification into energy channels is obtained. That means, beside the detection of the X-ray photons, additional information about its energy is generated and stored along with it.

To perform this photon counting and energy discriminating capability each pixel (100x100 µm²) may contain up to 2000 transistors. Offering several advantages (see *chapter 1.2*), this technology issues also several challenges to the electric circuits to make energy discrimination accurate. Mainly two effects have to be considered when determining energies of single photons:

- Pulse pile-up
- Charge sharing

Pulse pile-up describes the effect of two or more photons being detected within a single read-out cycle. This would result in distorted energy information linked to only one photon interaction. To reduce this effect, the dead-time is tuned to be short enough to make only single events appear within a cycle [2].

Charge sharing describes on the one hand the distribution of charge created by the incident photon which is spread over several pixels and on the other hand k-escape events within the crystal. Both effects lead to distorted energy information, as well, but in this case the energy is underestimated and distributed over neighbour pixels compared to the real energy of the interacting photon. Additionally, the inner unsharpness of the detector increases due to different detector elements reacting on only one interacting X-ray photon. To ensure high spatial and accurate energy resolution this effect needs to be corrected. PCDs by XCounter AB (Sweden) [1] are equipped with a built-in charge sharing correction which compares charges being spread over nearest neighbour pixels within a single read-out cycle and increases the counter only for the pixel with the highest individual charge. [2, 3]

1.2 Properties

In comparison to charge integrating detectors, PCDs have no read-out noise. Only if a charge pulse generated by a photon reaches a certain threshold, the event is being counted. As long as the threshold is higher than the noise of the electronics, the dark signal of the detector is zero. No read-out noise means no offset image to be corrected within a calibration. Stable long time measurements can be performed. Furthermore, the dynamic range of the detector is not limited by the bit-depth of the internal counter (e.g. 12- or 16-bit), as one can accumulate almost infinite number of frames without accumulating noise.

As consequence of the direct detecting semiconductor technology which renounces the scattering scintillation layer the basic spatial resolution (SR_b) is only limited by the pixel size. Any other sources for inner unsharpness are cancelled out at perpendicular angle of incidences (AoI). Under small AoIs the SR_b drops with increasing number of radiated pixels (see Figure 2).

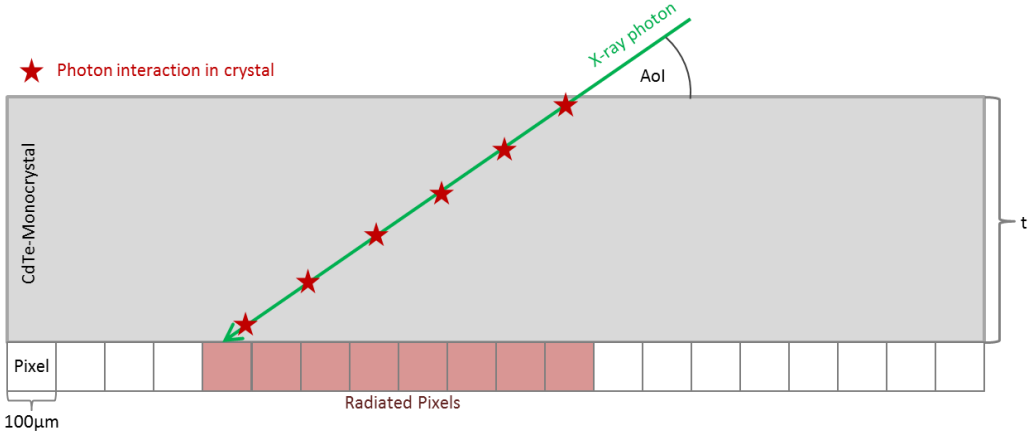

Figure 2: Pixel irradiation for small AoIs

For NDT purposes the image unsharpness (u_i) or basic spatial resolution (SR_b) is measured using duplex wire IQIs [4]. Figure 3 shows the expected $SR_b^{detector}$ in dependence on the AoI and thickness of the detection layer t which is of special importance for laminographic applications.

$$\frac{1}{2}u_i = SR_{b,expected}^{detector} = \frac{t_{crystal}}{\tan(AoI)} \quad (1)$$

and

$$SR_{b,min}^{detector} = SR_{b,pixel}^{detector} \quad (2)$$

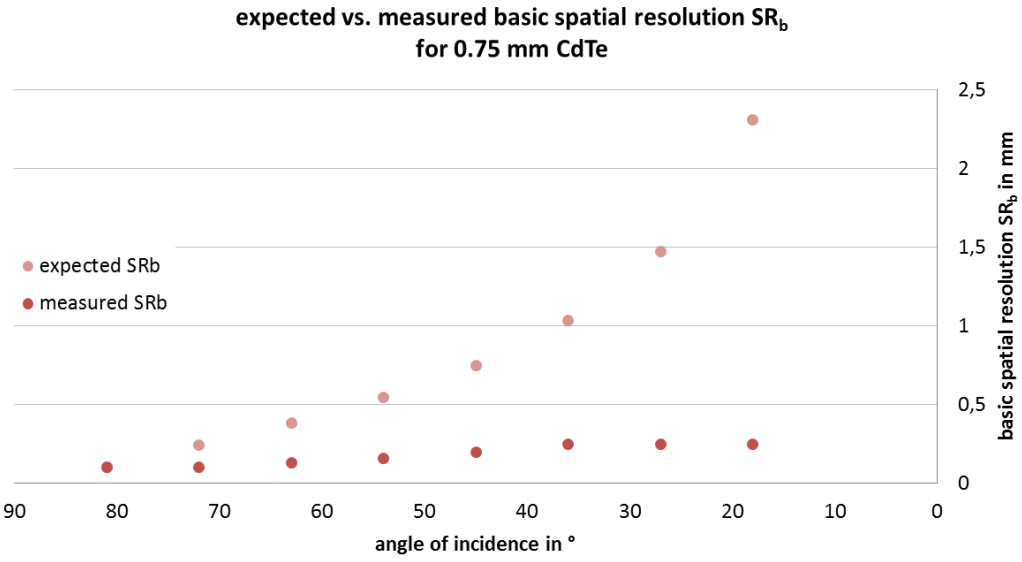

Figure 3: Expected vs. measured spatial resolution for different AoIs (pixel size = 0.1mm)

The expected SR_b increases with smaller AoIs whereas the measured SR_b doesn't exceed a limit of 0.25mm even under AoIs of about 18°. This enhanced resolution is another consequence of the charge sharing correction which compares exposed neighbour pixels before increasing the counts (see *chapter 1.1*).

The effect of the energy discriminating capability of the PCD on detected X-ray spectra is shown in Figure 4. When the energy of an incident photon is determined the count is given to one of two energy channels (*low* or *high*) with respect to the set thresholds. If the energy of the photon is lower than the first threshold (*Th1*) the photon will not be counted. That means it is possible to avoid low energetic scattered radiation to be detected which enhances the contrast sensitivity. On the other hand, when raising the first threshold counts are getting lost and SNR decreases.

When run in *dual-energy* mode (i.e. both threshold set) splitting the spectra like shown in Figure 4 enables the separation of materials within one single shot. Nevertheless, threshold optimization and advanced calibration procedures are necessary to optimize material decomposition.

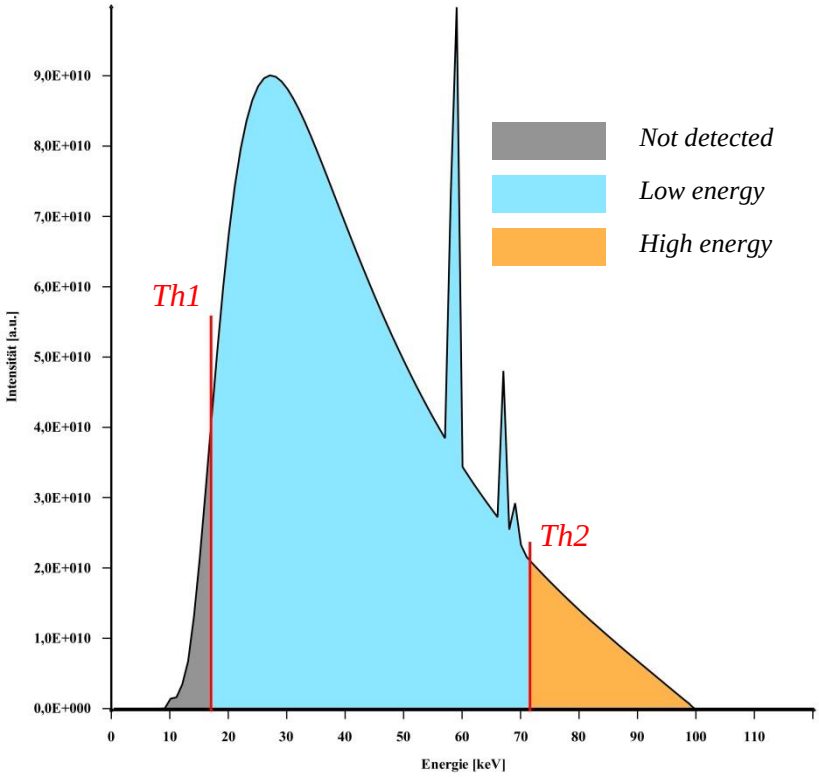

Figure 4: Selective detection of photons of a bremsspectrum (example) by thresholding inside of the detector

2. Applications

2.1 High Wall Thickness Measurements

As described in *chapter 1.1*, PCDs have no read-out noise i.e. no dark current. This property allows accumulating almost infinite no. of frames (depending on the calibration and temperature stabilization) which makes the PCD an ideal tool for long time measurements. High wall thickness pipes ($t_{wall} \geq 30\,mm$) like often used in (nuclear) power plants are hard to inspect with common RT methods in double wall technique. Inspecting pipes with Ir192 or Co60 gains very poor contrast in classical film radiography and mobile X-ray sources with energies above 300 keV are not available or not handy, respectively. This makes detection of very small indications extremely difficult with these techniques.

Within the EU-project TomoWELD [5] a mobile X-ray source was used at 270 kV in combination with a CdTe based PCD for inspecting high wall thickness pipes. The relatively low maximum energy of the X-ray source is compensated by the very efficient and long term stable PCD. The image shown in Figure 5 represents a high wall thickness measurement acquired with the parameters in Table 1. The bright white lines following the tile gaps and bright cluster pixels are insufficiently corrected bad pixels due to poor bad pixel mapping but they don't impair the results.

Table 1: Radiographic setup for high wall thickness measurement

Tube voltage	270 kV
Tube power	300 W
Source-detector distance	405 mm
Penetrated thickness	70 mm Fe
No. of frames (accumulated)	4,800
Exposure time per frame	0.5 s
Total exposure time	40 min
Total (photon) counts per pixel	~ 10,000
Counts per frame and pixel	~ 2

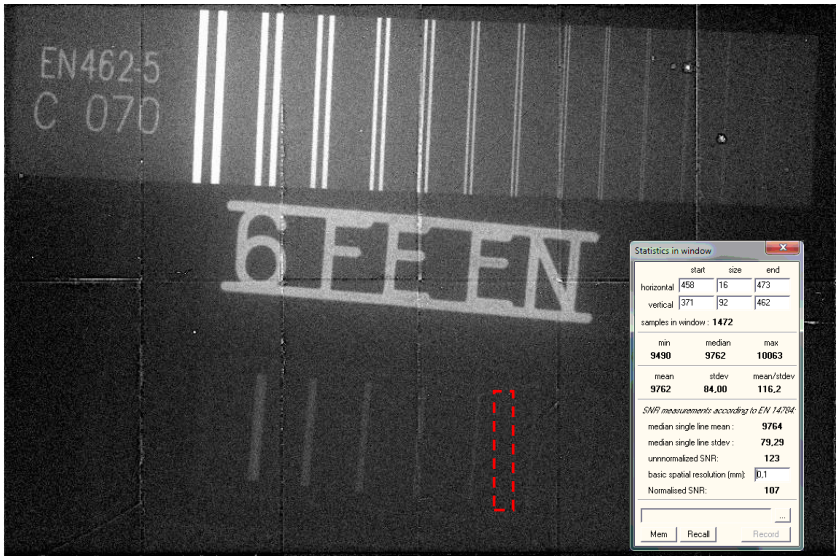

Figure 5: Double wall single image technique; 70 mm Fe; Image class B achieved[1]

Although the tube voltage of 270 kV seems to be insufficient to penetrate a thickness of 70 mm of steel (suggested voltage[1]: 600 kVp), all image quality criteria required for testing Class B[1] were fulfilled (see Table 2). This is even more surprising as in each single frame the averaged counts per pixel were approx. 2!

Table 2: Image quality in high wall thickness measurement

Image quality criterion	**Required**[1]	**Achieved**
Normalized signal-to-noise ratio (SNR_N)	70	107
Single wire (contrast sensitivity)	W10	W11
Duplex wire (SR_b)	D10 (0.1 mm)	D10 (0.1 mm)

[1] according to ISO 17636-2

2.2 Carbon Fibre Reinforced Plastics

With the increasing amount of CFRP structures used in aerospace or other industries the requirement for efficient and reliable NDT methods increases. The most common technique to investigate CFRP structures is ultrasound testing. But as each NDT method has its benefits and disadvantages, capabilities of ultrasound testing is limited regarding spatial resolution and searching for non-planar defects like undulations (Figure 6) or quantifying porosity and voids, respectively. [6]

With respect to their high basic spatial resolution and high dynamic range, investigating CFRP structures with X-rays, PCDs offer new opportunities for reliable and fast NDT especially in combination with laminographic techniques [7]. Figure 6 shows an undulation found in a CFRP sample acquired via "normal" radiography. The image was taken using a Si-based PCD (ModuPIX by ADVACAM) and an X-ray tube operating at 20 kVp and 160 W. After proper multi-gain calibration one can clearly see the fibre structure and especially the undulation in the middle of the image.

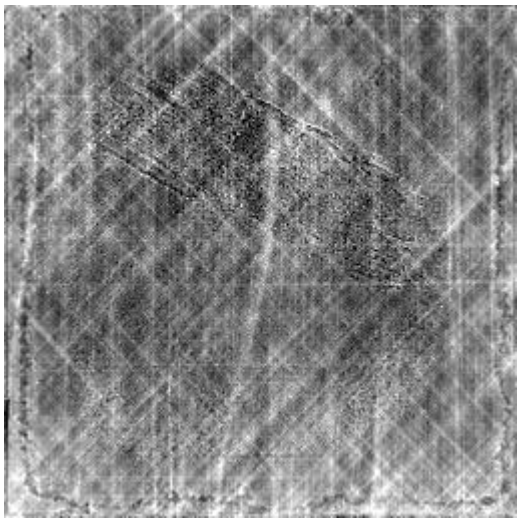

Figure 6: Undulation in CFRP sample (55 µm pixel pitch, Mag. = 1)

Figure 7 shows the results of a laminographic scan of a CFRP sample containing a variety of voids and porosity. The image represents the void volume of three CFRP samples manufactured under three different atmospheric pressures. This scan was done in order to evaluate the voids and porosity with respect to their size and quantity.

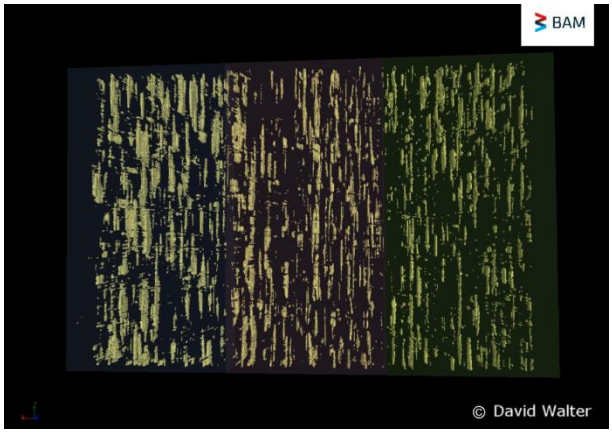

Figure 7: Laminographic results of CFRP samples containing voids and porosity

2.3 Dual Energy Imaging

Material discrimination using X-rays is based on the difference in energy dependency of the mass attenuation coefficient of the investigated materials [8]. Hence, images at different X-ray energies need to be acquired to discriminate materials. When two different energies are used, this technique is called *dual-energy imaging*. Common dual-energy imaging is achieved by acquiring two images at two different X-ray tube voltages (*dual-shot*), i.e. two distinct incident X-ray spectra.

The energy discriminating capability of the PCD enables separation of an incident X-ray spectrum into a low energy (*LE*) and high energy (*HE*) part by internal and selective energy thresholding (*single-shot*; see Figure 4).

Figure 8 shows two step wedges (Fe and Al) radiographed by dual energy technique. The dual energy image represents the solution of the dual energy function $F(Z)$ [9].

$$\mathrm{F(Z)} = \frac{\mu_{Low}(Z)}{\mu_{High}(Z)} = \left(\frac{\int_{E_1=0}^{E_{\max}} W(E_1)\,\mu(\mathrm{E}_1, Z)\,dE_1}{\int_{E_2=0}^{E_{\max}} W(E_2)\,\mu(\mathrm{E}_2, Z)\,dE_2} \right) \tag{3}$$

with

$$W(E) = \frac{S(E)\cdot D(E)}{\int_{E=0}^{E_{\max}} S(E)\cdot D(E)\,dE} \tag{4}$$

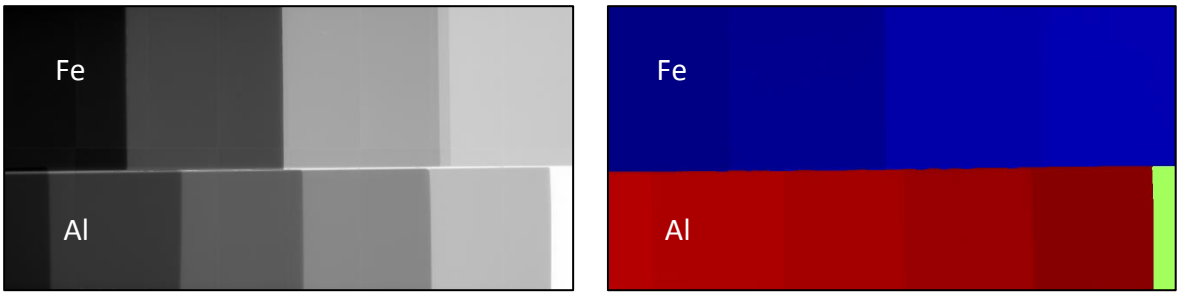

Figure 8: Radiographic image (left) taken at 160kV and dual energy image (right) of Fe and Al step wedges (green = free beam/air)

Low and *high* energy images were acquired using the internal energy thresholding of the PCD. The contrast enhancement between Al and Fe in the dual energy image is obvious and both materials can clearly be separated over the whole range of thicknesses.

Besides using the dual-energy function $F(Z)$ for materials discrimination, various other techniques (e.g. *inverse mapping*, *weighted logarithmic subtraction*) [8, 10, 11] are being investigated for NDE applications.

3. Conclusion

The benefits of PCDs are used in different application fields of NDT. No read-out noise and high dynamic range enable high wall thickness pipe inspection and very long term

measurements with low X-ray energy and therefore reduced controlled area. Even under conditions which are unsuitable for radiographic inspection with other detectors (low tube voltage and low power; high penetrated thickness; dense material) image quality class B (according to ISO 17636-2) can be achieved by accumulating numerous frames without adding additional noise.

Internal energy thresholds are used to split incident X-ray spectra and acquire dual-energy images which are used for material decomposition purposes. When only using one threshold, the influence of scattered radiation on the image quality can be reduced.

The implemented charge sharing correction increases the energy resolution and the spatial resolution, as well, which is very beneficial for tomosynthesis applications (e.g. laminography) especially under small AoIs.

Acknowledgements

The work presented in *chapter 2.1* has received funding from the European Union's Seventh Framework Programme for research, technological development and demonstration under grant agreement no 315213 for collaborative projects FP7-SME 2012 under "TomoWELD" ("*Development of Quantitative Radiographic Tomography technology for the in-situ Inspection of welded austenitic safety critical pipework in the nuclear power generation and petrochemical industries"*).

References

[1] XCounter AB, www.XCounter.com

[2] C. Ullberg, M. Urech, et al., *"Measurement of a Dual-Energy Fast Photon Counting CdTe Detector with integrated Charge Sharing Correction"*, Proc. SPIE 8668, Med. Imaging 2013

[3] K. Taguchi, J. Iwanczyk, *"Vision 20/20: Single photon counting x-ray detectors in medical imaging"*, Med. Phys. 40, 100901, 2013
http://scitation.aip.org/content/aapm/journal/medphys/40/10/10.1118/1.4820371

[4] ISO 17636-2:2013

[5] www.TomoWELD.eu

[6] M. Tartare, V. Rebuffel, et al., „*Dual and Multi-energy Radiography for CFRP Composites Inspection* "; Proc. 11th ECNDT, 2014, Prague, Proceedings
http://www.ndt.net/events/ECNDT2014/app/content/Paper/424_Rebuffel_Rev1.pdf

[7] U. Ewert, D. Fratscher et al., *„Laminographic Inspection of Fibre Composites and the Problem of Delaminations"*, 2nd International Symposium on NDT in Aerospace, 2010, Hamburg, Proceedings

[8] L. Lehmann, R. E. Alvarez, et al., *"Generalized image combinations in dual KVP digital radiography"*, Med. Phys. 8(5), pp.659 – 667, 1981

[9] S. Kolkoori et al., *„Dual High-Energy X-ray Digital Radiography for Material Discrimination in Cargo Containers"*, 11th ECNDT, 2014, Prague, Proceedings
http://www.ndt.net/events/ECNDT2014/app/content/Paper/149_Kolkoori_Rev1.pdf

[10] S. Cheenu Kappadath and Chris C. Shaw, *"Dual-energy digital mammography: Calibration and inverse-mapping techniques to estimate calcification thickness and glandular-tissue ratio"*, American Association of Physicists in Medicine 30(6), pp. 1110 – 1117, 2003

[11] H. Bornefalk et al., *"Single-shot dual-energy subtraction mammography with electronic spectrum splitting: Feasibility"*, Elsevier, European Journal of Radiology 60, pp. 275-278, 2006